

Understanding the Role of RNase III in *Mycobacterium smegmatis* RNA Metabolism

This report represents the work of one WPI undergraduate student submitted to the faculty as evidence of completion of a degree requirement. WPI routinely publishes these reports on the web without editorial or peer review.

A Major Qualifying Project

Worcester Polytechnic Institute

Samantha Joubran

Date: 03/18/2020

Project Advisor: Scarlet Shell, PhD

Project Co-Advisor: José Argüello, PhD

TABLE OF CONTENTS:

Abstract.....	1
Introduction.....	2
Methodology.....	7
Table 1: Plasmids.....	7
Table 2: Bacterial Strains.....	7
Table 3: qPCR Oligo Primers.....	8
Table 4: qPCR Thermocycler Program.....	8
Table 5: RNA Extraction DNase 1X Master Mix.....	10
Table 6: cDNA Synthesis 1X RT Master Mix.....	11
Table 7: cDNA Synthesis 1X no-RT Master Mix.....	11
Table 8: qPCR Thermocycler Program.....	11
Table 9: 5' RACE Oligo Primers.....	12
Table 10: Adapter Ligation 1X Master Mix.....	13
Table 11: Taq PCR 1X Master Mix.....	14
Table 12: Taq PCR Thermocycler Program.....	14
Table 13: Primer Pair Annealing Temperatures.....	14
Table 14: 3' RACE Oligo Primers.....	15
Table 15: Adapter Ligation 1X Master Mix.....	16
Table 16: Primer Pair Annealing Temperatures.....	16
Results.....	17
Figure 1.....	18
Figure 2.....	19
Figure 3.....	20
Figure 4.....	21
Figure 5.....	21
Figure 6.....	22
Figure 7.....	23
Figure 8.....	24
Figure 9.....	25
Figure 10.....	25
Figure 11.....	26
Figure 12.....	27
Figure 13.....	28
Figure 14.....	28
Discussion.....	29
References.....	32

ABSTRACT:

Mycobacterium tuberculosis causes 1.4 million deaths world-wide every year (World Health Organization, 2020). An important aspect of the bacteria's ability to survive environmental or antibiotic stressors is its regulation of RNA metabolism. Ribonuclease III is an enzyme that cleaves double-stranded RNA. In some bacteria, it plays an important role in mRNA degradation as well as tRNA and rRNA maturation. It is an essential gene in *Mycobacterium smegmatis*, a non-pathogenic model for *Mycobacterium tuberculosis*, and this project focused on understanding this essentiality in the context of mRNA degradation and rRNA maturation. Potential RNase III mRNA cleavage sites were determined and the expression levels of the genes flanking these sites were quantified when RNase III was knocked down. The initial studies showed that RNase III had no effect on the expression of the genes flanking these sites. The focus of the project shifted to examining the role of RNase III in rRNA maturation. RNA agarose gels of samples where RNase III was knocked down showed new bands at around 5,000 base pairs appearing and a suspected pre-16S rRNA band disappearing compared to the control samples. 5' RACE and 3' RACE experiments confirmed the presence of a cleavage site 151 bp upstream of the 16S rRNA gene (MSMEG_3757) and another cleavage site 212 bp upstream of the 23S rRNA gene (MSMEG_3756); both are hypothesized to be done by RNase III. Additionally, these experiments identified the location of another cleavage site 150 bp upstream of the 23S rRNA gene, which is likely the result of RNase E. Further testing will need to be done in order to confirm that these sites are cleaved by RNase III and RNase E.

INTRODUCTION:

Tuberculosis is a worldwide epidemic caused by infection with *Mycobacterium tuberculosis* (World Health Organization, 2020). This is primarily a problem in developing countries where tuberculosis is more common. Approximately 1.4 million people die every year because of tuberculosis and it is one of the top 10 causes of death worldwide (World Health Organization, 2020). Around 500,000 cases a year are caused by *M. tuberculosis* that is resistant to rifampicin (one of the best antibiotics for treating *M. tuberculosis*) and of those, 78% are multi-drug resistant (World Health Organization, 2020). *M. tuberculosis* is spread through aerosolized droplets that enter human lungs and are engulfed by resident macrophages. Inside the macrophages, the vesicles containing the bacteria, known as phagosomes, are fused with the lysosome, which subjects the bacteria to stressful conditions such as hypoxia, acidic pH, reactive oxygen or nitrogen species, and other toxins (Smith, 2003). Other immune cells are signaled to the site of infection and they form a granuloma around the infected cells (Smith, 2003). However, if the infected individual's immune system is weakened, the bacteria can escape and be released in droplets into the air (Smith, 2003).

In order to develop more effective antibiotics for treating tuberculosis, scientists study how *M. tuberculosis* functions and what mechanisms it employs to survive the harsh conditions of the macrophage in order to better understand how to target these bacteria. In order to study tuberculosis, scientists often examine *Mycobacterium smegmatis*, which is closely related but is non-pathogenic since *M. tuberculosis* is a highly contagious and pathogenic microbe. One

important factor that aids *M. tuberculosis* in adapting to changes in its environment is RNA metabolism (Arraiano, 2010).

Ribonucleases (RNases) play an important role in the regulation, maturation, processing, and degradation of RNA that is transcribed in cells. There are two main types of RNases: endoribonucleases and exoribonucleases (Nicholson, 1999). Endoribonucleases cleave RNA phosphodiester bonds in the middle of an RNA sequence (Nicholson, 1999). Exoribonucleases cleave RNA phosphodiester bonds from the 3' or 5' ends of the sequence (Nicholson, 1999). These enzymes play an important role in the maturation and processing of tRNA and rRNA along with the degradation of mRNA and ultimately the other types of RNAs. This cycle of RNAs being processed by RNases and ultimately degraded by RNases allows cells to be able to respond to changes in their environment (Nicholson, 1999).

In organisms like *E. coli* and *Mycobacterium smegmatis*, there are different RNases such as RNase E that cleave single stranded mRNA and rRNA (Taverniti, 2011). However, RNase E and RNase J cannot cleave double-stranded RNA and they preferentially process RNAs with 5'-monophosphate ends (Mackie, 1998 and De La Sierra-Gallay, 2008). In 2011, Taverniti and colleagues hypothesized that another RNase was involved in the initial processing of double-stranded RNA in *Mycobacterium smegmatis*. Based on the secondary structure of the RNA and the presence of an RNase in the *Mycobacterium smegmatis* genome with sequence homology to the *E. coli* RNase III, this other RNase is presumed to be part of the RNase III family of enzymes. Therefore, RNase III is predicted to play a role in rRNA maturation in *Mycobacterium smegmatis*.

RNase III enzymes are homodimers that cleave double-stranded RNA and leave two-nucleotide overhangs on the 3' ends of each RNA strand (Ji, 2008). RNase III enzymes depend

on a divalent metal cation cofactor, usually magnesium, in order to function (Conrad, 1998) and homologues are found in most organisms from humans to viruses (Altuvia, 1987). In bacteria, RNase III has two important domains: an endonuclease domain (involved in catalysis) and a double-stranded RNA binding domain (dsRBD) (Lee, 2003; Ji, 2008; Calin-Jageman, 2003).

In *Bacillus subtilis*, RNase III is essential for the bacteria to degrade *txpA* and *yonT*, which come from Skin and SP β , two prophages (Durand, 2012). These genes code for toxins to aid the prophages in infection of the hosts. In *Staphylococcus aureus*, RNase III is involved in the maturation of tRNA and rRNA, degradation of mRNA and ncRNA (non-coding RNA), and the regulation of its translation (Lioliou, 2012). In *E. coli*, RNase III cleaves the 5' UTR of its own transcript in order to initiate its degradation and regulate the RNase III levels in the cells. In *E. coli*, RNase III is involved in the processing of mRNA transcripts containing key metabolic enzymes. In some cases, RNase III processing initiates the degradation of the mRNA and in other cases it stabilizes the mRNA (Gordon, 2017). For example, RNase III is responsible for initiating the degradation of *corA*, which codes for a metal ion transporter for cobalt, magnesium, and nickel (Lim, 2012). As a result, the concentrations of these metals in the *E. coli* cells change upon changes in RNase III concentrations.

Studies have found that RNase III in *E. coli* is not sequence specific (Zhang, 1997; Nicholson, 1999). The cleavage sites are determined by where RNase III binds to the RNA. It is not very well known why RNase III binds to those sites in order to cleave the RNA. If unfavored Watson-Crick base pairs are introduced in locations where RNase III typically binds to RNA, then RNase III binding is inhibited (Zhang, 1997). It has also been found that the presence of a bulge, loop, or bulge motif in the secondary structure of RNA inhibits RNase III binding (Calin-Jageman, 2003). A bulge loop or bulge motif is a segment of an RNA hairpin loop where the

nucleotides cannot form a helix because the bases on the two RNA strands cannot base pair together.

RNase III has been largely studied in *E. coli* where it has two main functions: the maturation of rRNA and the degradation of mRNA (Nicholson, 1999; Bardwell, 1989; Verma, 1994). In *Mycobacterium smegmatis*, rRNA is transcribed on a polycistronic transcript containing the genes for the 23S, 16S, and 5S rRNA. The transcript is comprised of a leader sequence, the 16S rRNA (MSMEG_3757), a spacer region, the 23S rRNA (MSMEG_3756), another spacer region, the 5S rRNA (MSMEG_3755), and a terminator sequence (shown in Figure 5) (Taverniti, 2011). RNase III was proposed to process the transcript within the leader sequence, twice in the first spacer region, and once in the second spacer region (Taverniti, 2011). These processing sites were identified by primer extension assays when RNase E, RNase J, or both were knocked down. Other enzymes such as RNase E and RNase J process the 23S, 16S, and 5S rRNA into their mature forms (Taverniti, 2011). In *E. coli* mRNA degradation, RNase III cleaves transcripts upstream of the coding sequence (Bardwell, 1989). This de-stabilizes the mRNA and leads to further mRNA degradation by other enzymes (Bardwell, 1989; Altuvia, 2018). However, the role of RNase III in mycobacterial mRNA degradation has not been previously investigated.

In order to better understand RNase III's role in RNA metabolism in mycobacteria, this project studied *Mycobacterium smegmatis* as a model for *Mycobacterium tuberculosis*. We focused on determining the role of RNase III in *M. smegmatis* degradation of double-stranded mRNA (such as the stem of a hairpin loop) and the maturation of rRNA transcripts. The data presented here showed no conclusive evidence about whether RNase III is involved in the degradation of some mRNAs. However, our 3' RACE and 5' RACE experiments confirmed the

presence of cleavage sites hypothesized in Taverniti *et al.*, 2011 and refined the locations of these sites; further experiments are still required to confirm that RNase III is the enzyme responsible for these cleavage sites.

METHODOLOGY:

Strain Construction:

Strains SS-M_0203, SS-M_0204, and SS-M_0205 were previously designed by another Shell lab member (see Tables 1 and 2 for details). In previous experiments, primers were designed to amplify the CRISPRi plasmid and replace the non-specific sgRNA with sgRNA specific for MSMEG_2418, creating plasmid pSS400. The plasmid pSS400 was transformed into *Mycobacterium smegmatis*. Three transformed colonies were collected to make strains SS-M_0715, SS-M_0716, and SS-M_0717, which were stored at -80°C.

Table 1: Plasmids

Plasmid Name	Details
pJR962 (Rock, 2017)	CRISPRi construct with dCas9 and non-specific sgRNA
pSS400	CRISPRi construct with dCas9 and sgRNA to bind to MSMEG_2418

Table 2: Bacterial Strains

Strain Name	Details
SS-M_0203	<i>Mycobacterium smegmatis</i> strain mc ² 155 transformed with pJR962
SS-M_0204	<i>Mycobacterium smegmatis</i> strain mc ² 155 transformed with pJR962
SS-M_0205	<i>Mycobacterium smegmatis</i> strain mc ² 155 transformed with pJR962
SS-M_0715	<i>Mycobacterium smegmatis</i> strain mc ² 155 transformed with pSS400 to knockdown MSMEG_2418
SS-M_0716	<i>Mycobacterium smegmatis</i> strain mc ² 155 transformed with pSS400 to knockdown MSMEG_2418
SS-M_0717	<i>Mycobacterium smegmatis</i> strain mc ² 155 transformed with pSS400 to knockdown MSMEG_2418

Designing qPCR Primers:

qPCR primers were designed using the Primer Quest tool from IDT and tested to determine if they had high efficiency and specificity for the target regions. A five-fold dilution series of *M. smegmatis* cDNA was made and run with a 2.5 µM solution of the primers and iTaq Universal Sybr Supermix. The 96 well plate was run according to the qPCR Thermocycler

settings in Table 4. Primer sets were considered acceptable if their melting curves only had one peak and no shoulders, and the amplification efficiency was between 85 and 100% (efficiency was calculated by finding $10^{-1/\text{slope}} - 1$, the slope referred to the line of best fit of the \log_{10} cDNA concentration versus the C_T value).

Table 3: qPCR Primers

Primer Name	Function	Sequence
JR273	Forward qPCR primer for MSMEG_2758	GACTACACCAAGGGCTACAAG
JR274	Reverse qPCR primer for MSMEG_2758	TTGATCACCTCGACCATGTG
SSS2058	Forward qPCR primer for MSMEG_2080	GTGATCAACGGCGAGAAGAT
SSS2059	Reverse qPCR primer for MSMEG_2080	GGCACGATGAACGACTTGA
SSS2062	Forward qPCR primer for MSMEG_2079	GAATCGTTTCAGGCATTGGTG
SSS2063	Reverse qPCR primer for MSMEG_2079	CTTGAAGTTCACGCTGGAGTA
SSS2066	Forward qPCR primer for MSMEG_5999	CCACTTCGCCACCATGAA
SSS2067	Reverse qPCR primer for MSMEG_5999	CACCGGAACTCGTGTTGAT
SSS2070	Forward qPCR primer for MSMEG_5998	GAACGTCTCAACGCCAAATC
SSS2071	Reverse qPCR primer for MSMEG_5998	CTTCCCGTTGGTGGTCTT
SSS2080	Forward qPCR primer for MSMEG_6007	TCGACGTGAGACGGATGTAA
SSS2081	Reverse qPCR primer for MSMEG_6007	AATTAAGCATGCGGATCGTG
SSS2102	Forward qPCR primer for MSMEG_6008	CAGCAGGCCATTTTCCTTTG
SSS2103	Reverse qPCR primer for MSMEG_6008	GTGCTGAATCCGAGTTCCTT
SSS2150	Forward qPCR primer for MSMEG_2418	CCTCTTGGGTGCAATCTATCTC
SSS2151	Reverse qPCR primer for MSMEG_2418	GTTCTGCAGACTGCTCTT

Table 4: qPCR Thermocycler Program

Step	Temperature (°C)	Time
Holding Stage	50	2 minutes
Holding Stage	95	10 minutes
Cycling Stage	95	15 seconds
	61	1 minute
	*This stage was repeated for 40 cycles	
Melting Curve Stage	95	15 seconds
	60	1 minute
	95	30 seconds
	60	15 seconds

Growth Media:

Cultures were grown in 7H9 broth made by mixing 7.05 g of Difco Middlebrook 7H9, 7.5 g of BSA Fraction V, and 1475 mL of ultra-pure water and heating the solution until dissolved. Six milliliters of 50% glycerol, 3.75 mL of 20% Tween 80, and 15 mL of 100X albumin dextrose catalase (ADC) were added and the solution was filter sterilized.

Growth curves:

Aliquots of frozen cultures were grown in 7H9 with 25 µg/mL of kanamycin at 37°C and 200 rpm. The optical densities (ODs) of the cultures were measured and the cultures were diluted in duplicate to ODs of 0.01. One duplicate of each culture had anhydrotetracycline (ATc) added to a final concentration of 200 ng/mL. Cultures were incubated for 11 hours at 37°C and shaking at 200 rpm. After 11 hours, ODs were measured every hour and a half until the cultures with ATc and RNase III knockdown stopped growing.

RNA Extractions and Purification:

The ODs of the cultures were measured before they were centrifuged at 3,900 rpm and 4°C for 5 minutes. The supernatant was removed and then the cultures were centrifuged again for 1 minute and the remaining supernatant was removed with a pipette. The pellets were resuspended in 1 mL of TRIzol and transferred to OPS Diagnostics 100 µM zirconium lysing matrix tubes. The tubes were subject to bead-beating in an MP Bio FastPrep 5G for 3 cycles of 7 m/s for 30 seconds with 2 minutes on ice between cycles. Three hundred microliters of chloroform was added to each sample and the samples were vortexed for 15 seconds. The samples were centrifuged at 15,000 rpm and 4°C for 15 minutes. Five hundred microliters of the aqueous layer of each sample were mixed with 500 µL of 100% ethanol. The samples were

added to columns and centrifuged at 15,000 rpm and room temperature for 30 seconds. RNA was purified with a Direct-zol RNA MiniPrep kit (Zymo) according to the manufacturer's instructions and then stored at -80°C.

Table 5: RNA Extraction DNase 1X Master Mix

Reagent	Amount
DNase Digestion Buffer	75 μ L
DNase I	5 μ L
Total	80 μ L

cDNA Synthesis and Purification:

RNA samples were diluted in duplicate to 600 ng. One microliter of the random primer mix, containing 83% 100 mM Tris pH 7.5 and 17% 3 mg/mL NEB random primers, was added to each sample. The samples were incubated at 70°C for 10 minutes and then cooled in an ice bath for 5 minutes. RT and no-RT master mixes were made as detailed in Tables 6 and 7. Three and seventy-five hundredth microliters of the RT master mix was added to one of the duplicates for each sample and 3.75 μ L of the no-RT master mix was added to the other. The samples were incubated at 25°C for 10 minutes, 42°C for 2.5 to 5 hours, and then stored at 4°C.

Ten microliters of a solution of 1:1 0.5 mM EDTA and 1M NaOH was added to each sample and the samples were incubated at 65°C for 15 minutes. Twelve and five tenth microliters of 1M Tris-HCL at a pH of 7.5 was added to each sample. cDNA was purified with a PCR & DNA Cleanup kit (Monarch) according to the manufacturer's instructions and then stored at 4°C.

Table 6: cDNA Synthesis 1X RT Master Mix

Reagent	Amount
ProtoScript II Buffer (5X)	2 μ L
dNTPs Mix (10 mM)	0.5 μ L
100 mM DTT	0.5 μ L
RNase Inhibitor, Murine, NEB (40,000 U/mL)	0.25 μ L
ProtoScript II Reverse Transcriptase, NEB (200,000 U/mL)	0.5 μ L
Total	3.75 μ L

Table 7: cDNA Synthesis 1X no-RT Master Mix

Reagent	Amount
ProtoScript II Buffer (5X)	2 μ L
dNTPs Mix (10 mM)	0.5 μ L
100 mM DTT	0.5 μ L
RNase Inhibitor, Murine, NEB (40,000 U/mL)	0.25 μ L
Ultra-Pure Water	0.5 μ L
Total	3.75 μ L

Quantitative PCR:

The synthesized cDNA for the RT was diluted to 200 pg/ μ L and the no-RT samples were diluted with the same volumes of water as the corresponding RT samples. Primer mixes were made by diluting the forward and reverse primers in a primer set in ultra-pure water so that they were both 2.5 μ M. Master Mixes for each primer set were made as described earlier. Two microliters of each cDNA dilution and 8 μ L of each master mix were added to a 96 well plate for each combination of conditions. The cDNA from the no-RT samples were only tested with the master mix with the qPCR primers for MSMEG_2758 (this acted as a control). The 96 well plate was run according to the qPCR Thermocycler settings in Table 8.

Table 8: qPCR Thermocycler Program

Step	Temperature ($^{\circ}$ C)	Time
Holding Stage	50	2 minutes
Holding Stage	95	10 minutes
Cycling Stage	95	15 seconds

	61	1 minute
*This stage was repeated for 40 cycles		

RNA Gel Electrophoresis:

RNA was run on 1% TBE-agarose gels. RNA samples were diluted to 300 ng in a 6 μ L. Six microliters of 2X RNA loading dye was added to each sample and the samples were heated at 65°C for 5 minutes. Gels were run for 40 minutes at 145 volts.

5' RACE:

Table 9: 5' RACE Oligo Primers

Primer Name	Function	Sequence
SSS1016	Shortened Invitrogen GeneRacer 5' RNA Oligo Adapter	CTGGAGCACGAGGACACTGACA TGGACTGAAGGAGTrArGrArArA
SSS1017	Shortened Invitrogen GeneRacer 5' DNA Oligo Primer	CTGGAGCACGAGGACACTGA
SSS1018	Shortened Invitrogen GeneRacer 5' DNA Nested Oligo Primer	CTGACATGGACTGAAGGAGTA
SSS2209	Reverse Primer for 5' RACE ~60 nt upstream of 16S rRNA (MSMEG_3757) to map putative RNase III cleavage site 1	TCTGACCTAACAAAACGACACC
SSS2210	Reverse Primer for 5' RACE ~50 nt upstream of 23S rRNA (MSMEG_3756) start to map putative RNase III cleavage site 3	AATTGCACATCAATTTGTCCGC
SSS2239	Nested Reverse Primer for 5' RACE ~90 nt upstream of 16S rRNA (MSMEG_3757) to map putative RNase III cleavage site 1	AACTGGCATCAAAAACATCCACC

RppH Treatment:

Two reactions with 1 μ g of RNA were prepared for each sample: one reaction with the pyrophosphohydrolase (RppH) treatment and one without the RppH treatment. The samples were incubated in a thermocycler at 37°C for 1 hour and then stored on ice. The samples were then purified with the 5 RNA Clean & Concentrator Kit (Zymo) according to the manufacturer's instructions.

Adapter Ligation:

The samples were diluted to 8 μL and the maximum possible concentration based on the concentrations of the samples after RppH treatment (usually concentrations ranging from 40-70 $\text{ng}/\mu\text{L}$). The samples were mixed with 1 μL of 10 μM primer SSS1016 and incubated for 10 minutes at 65°C before being kept on ice for 5 minutes. Twenty-one microliters of the adapter ligation master mix described in Table 10 was added to each sample. The samples were incubated at 20°C for 15-20 hours. The samples were then purified with the 5 RNA Clean & Concentrator Kit (Zymo) according to the manufacturer's instructions.

Table 10: Adapter Ligation 1X Master Mix

Reagent	Amount
50% PEG8000	10 μL
10X T4 RNA Buffer	3 μL
10 mM ATP	3 μL
100% DMSO	3 μL
Murine RNase Inhibitor	1 μL
T4 RNA Ligase	1 μL
RNA and SSS1016	9 μL
Total	30 μL

cDNA Synthesis and Purification:

Two reactions were prepared for each sample: one with RT and one without RT. One microliter of a primer mix consisting of 50% 100 mM Tris pH 7.5, 17% 3 mg/mL NEB random primers, and 33% RNase free water, was added to each reaction for each sample. The procedure for cDNA synthesis and purification described earlier was repeated with these samples from the incubation at 70°C for 10 minutes and on.

Taq Polymerase Chain Reaction (PCR):

The Taq PCR master mix described in Table 11 was made for the samples. Twenty-three and five tenth microliters of the master mix was added to PCR tubes (one for each reaction being run) and 1.5 μL of the corresponding cDNA template was added. The samples were run in a thermocycler following the conditions described in Table 12 and the annealing temperatures used are described in Table 13.

Table 11: Taq PCR 1X Master Mix

Reagent	Amount
10X Standard Taq Buffer	2.5 μL
10 μM Forward Primer	1.25 μL
10 μM Reverse Primer	1.25 μL
10 μM dNTPs	0.5 μL
100% DMSO	1.25 μL
Taq Polymerase	0.167 μL
DNA Template	1.5 μL (concentration varies from 5-15 ng/ μL)
Water	16.583 μL
Total	25 μL

Table 12: Taq PCR Thermocycler Program

Temperature ($^{\circ}\text{C}$)	Time	
95	5 minutes	
95	30 seconds	35 to 40 Cycles
Annealing Temp.	20 seconds	
68	25 seconds	
68	5 minutes	
4	Forever	

Table 13: Primer Pair Annealing Temperatures

Primer Pair	Annealing Temperature
SSS1017 & SSS2209	52 $^{\circ}\text{C}$
SSS1018 & SSS2239	50 $^{\circ}\text{C}$
SSS1017 & SSS2210	52 $^{\circ}\text{C}$

DNA Gel Electrophoresis:

The DNA was run on a 1.5% TAE-agarose gel. The samples were mixed with 6X DNA loading dye to create final solutions of 1X DNA loading dye. Ethidium bromide was added to the buffer before the gels were run for 30 minutes at 110-130 volts.

DNA Gel Extraction:

The DNA bands of interest were visualized using UV light and excised with a razor. The DNA was purified from the gel using a Zymoclean Gel DNA Recovery Kit following the manufacturer's instructions.

DNA Sequencing:

For samples with poor amplification of the desired DNA regions, the DNA was extracted as described above and then PCR, gel electrophoresis, and gel extraction were repeated with nested primers for the region of interest. After the desired bands were visualized on agarose gels, the extracted DNA was sent to Quintarabio for Sanger sequencing with the corresponding reverse primers.

3' RACE:

Table 14: 3' RACE Oligo Primers

Primer Name	Function	Sequence
SSS413	3' RNA Oligo Adapter with a 5' monophosphate and 3' dideoxynucleotide	AGAUCGGAAGAGCGUCGUGUAGGGA
SSS414	3' DNA Oligo Primer	TCCCTACACGACGCTCTTCCGATCT
SSS2240	Forward Primer for 3' RACE ~280nt upstream of 16S rRNA (MSMEG_3757) start to map putative RNase III cleavage site 1	GAAGCGAAGACAAAGTCCGAGAGAG
SSS2241	Forward Primer for 3' RACE 2nt downstream of 16S rRNA (MSMEG_3757) end to map putative RNase III cleavage site 2	GGAGCACCACGAGAGACACTCTCCG

Adapter Ligation:

Three microliters of the RNA samples at 500 ng/ μ L were mixed with 3 μ L of 10 μ M SSS413. The RNA-primer mixes were incubated at 65°C for 5 minutes before being chilled on ice for 1 minute. Twenty-six microliters of the adapter ligation master mix described in Table 15 was mixed with 4 μ L of each sample. The samples were incubated at 17°C for 15-20 hours. The samples were then purified with the 5 RNA Clean & Concentrator Kit (Zymo) according to the manufacturer's instructions.

Table 15: Adapter Ligation 1X Master Mix

Reagent	Amount
50% PEG8000	15 μ L
10X T4 RNA Buffer	3 μ L
10 mM ATP	3 μ L
100% DMSO	3 μ L
Murine RNase Inhibitor	1 μ L
T4 RNA Ligase	1 μ L
RNA and SSS413	4 μ L
Total	30 μ L

cDNA Synthesis and Purification:

Two reactions were prepared for each sample: one with reverse transcriptase and one without. One microliter of a primer mix containing 50% 100 mM Tris pH 7.5, 17% 10 μ M SSS414, and 33% RNase free water, was added to each reaction for each sample. The procedure for cDNA synthesis and purification described earlier was repeated with these samples from the incubation at 70°C for 10 minutes and on.

Taq PCR, DNA Gel Electrophoresis, DNA Gel Extraction, DNA Sequencing:

The protocols for Taq PCR, DNA Gel Electrophoresis, DNA Gel Extraction, and DNA Sequencing described for 5' RACE were repeated with the samples from 3' RACE.

Table 16: Primer Pair Annealing Temperatures

Primer Pair	Annealing Temperature
SSS2240 & SSS414	57°C
SSS2241 & SSS414	57°C

RESULTS:

RNase III is Essential in M. smegmatis:

RNase III was predicted to be essential in *Mycobacterium tuberculosis* and *Mycobacterium smegmatis* by TnSeq (DeJesus, 2017 and Eric Rubin, personal communication). To confirm this prediction and study its role, we therefore used CRISPRi to knockdown the expression of *rnc* (MSMEG_2418), the gene that codes for RNase III, in *Mycobacterium smegmatis* (Rock, 2017). Growth assays of the different cultures were run in order to determine that RNase III was essential for the bacteria and determine the point at which growth of the mutant with RNase III knocked down diverged from the controls. Four conditions were run: Non-Specific sgRNA, Non-Specific sgRNA +ATc, RNase III sgRNA, and RNase III sgRNA +ATc. Each condition had three biological replicates (see Table 2 for more details) and the CRISPRi plasmid transcription was induced by the addition of ATc. Figure 1A shows that over the course of 24 hours, the silencing of RNase III led to a plateau in growth. We therefore confirmed that *rnc* was essential for *Mycobacterium smegmatis* growth.

Growth of RNase III KD Cultures Diverge from Controls at 14 Hours and Plateau at 18 Hours:

The plate reader used to assess the growth of the cultures in Figure 1A analyzed samples of 200 μ L; however, further experiments required growth of 5 mL cultures in 50 mL tubes. Therefore, the conditions, in terms of available oxygen and nutrients, were different from the conditions of the samples tested in the plate reader. In order to get more accurate data about

when the growth of the mutant cultures diverged from the controls and plateaued, we used a bench-top spectrophotometer to measure growth of cultures in 50 mL tubes. Because all the controls behaved the same (Figure 2A), only one control was used for this experiment. The RNase III KD +ATc culture began to diverge from the control approximately 14 hours after ATc was added (Figure 1B). The growth continued to slow until approximately 18 hours after the addition of ATc when the growth appeared to fully plateau.

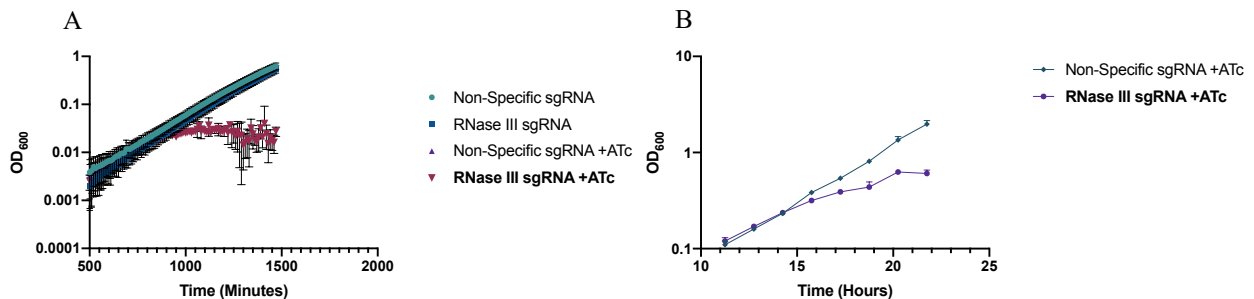


Figure 1: RNase III is Essential for Growth of *Mycobacterium smegmatis*.

A. The optical densities of *Mycobacterium smegmatis* cultures in a 96-well plate were measured every ten minutes in a combined shaker/incubator/plate reader. **B.** The optical densities of *Mycobacterium smegmatis* cultures grown in 50 mL conical tubes were measured every hour by a bench-top spectrophotometer. Note the pathlengths of the two instruments were different. The data shown here are the mean and standard deviation of triplicate biological replicates.

CRISPRi is Effective at Decreasing the Expression of *rnc*:

Quantitative PCR (qPCR) was used to determine how effectively CRISPRi silenced the expression of *rnc* in order to better understand the results of the next experiments. The RNA of the cultures was extracted at 12 hours (before growth of RNase III sgRNA +ATc diverged) and 18 hours (after growth of RNase III sgRNA +ATc stopped). The expression level of *sigA* was determined for all the cultures and used to normalize the expression level of *rnc*. Figure 2 shows that even before the growth of RNase III sgRNA +ATc diverges from the controls, there is a significant 15-fold decrease in the expression of *rnc* in these cultures compared to the controls. After growth of RNase III sgRNA +ATc stops, there is a 37-fold decrease in the expression of

rnc in these cultures compared to the controls. Additionally, the expression of *rnc* in RNase III sgRNA +ATc at 18 hours is significantly less than the expression of it at 12 hours.

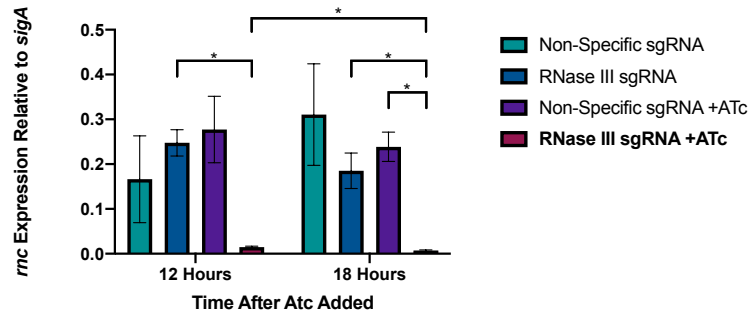


Figure 2: CRISPRi Decreases the Expression of *rnc*.

Expression in triplicate cultures was measured by qPCR at the indicated times following addition of ATc. Bars shown mean and error bars denote standard deviation. * denotes $p < 0.05$.

Identifying Potential RNase III mRNA Targets:

Martini *et al.* (2019) previously mapped the 5' ends of RNA transcripts in *Mycobacterium smegmatis*. Within this dataset, we identified a few likely cleavage sites (5' ends with 5' monophosphates instead of 5' triphosphates) that did not appear to be attributable to RNase E because they lacked the sequence motif common to RNase E cleavage sites. These sites were compared with sites containing the Tuberculosis Rho-independent terminator motif as described by Gardner *et al.* (2011). The sites that were located within Tuberculosis Rho-independent terminator motifs were likely to be double-stranded and therefore, likely RNase III targets. Three potential RNase III cleavage sites that met both criteria were identified: between MSMEG_2080 and MSMEG_2079, between MSMEG_5999 and between MSMEG_5998, and MSMEG_6008 and MSMEG_6007 (Figure 3).

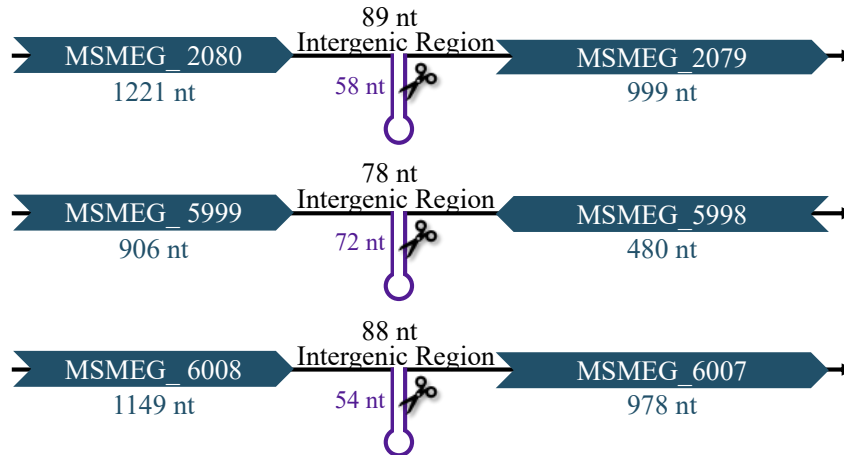


Figure 3: Possible RNase III mRNA Targets.

The graphic shows the three potential RNase III cleavage sites as the cartoon scissors. The purple hairpin loops represent TRIT sequences (Gardner *et al.* 2011) and the blue regions represent the genes flanking the potential cleavage sites.

RNase III Knockdown Did Not Affect the Expression Levels of the Genes Flanking Putative

RNase III Cleavage Sites:

We used Quantitative PCR to measure the expression of the genes flanking the sites of interest to gain insight about how the silencing of *rnc* affected them. RNA was extracted from cultures 12 hours after ATc addition, since 12 hours is before the growth of the bacteria stops and the effects of RNase III can be visualized without being confounded by changes in RNA regulation or degradation due to the bacterial growth slowing. Figure 4 shows that the silencing of RNase III did not affect the expression levels of the genes. The controls and the RNase III sgRNA +ATc cultures had expression levels that were not significantly different. Therefore, RNase III does not appear to play a role in determining the expression levels of MSMEG_2080, MSMEG_2079, MSMEG_5999, MSMEG_5998, MSMEG_6008, and MSMEG_6007.

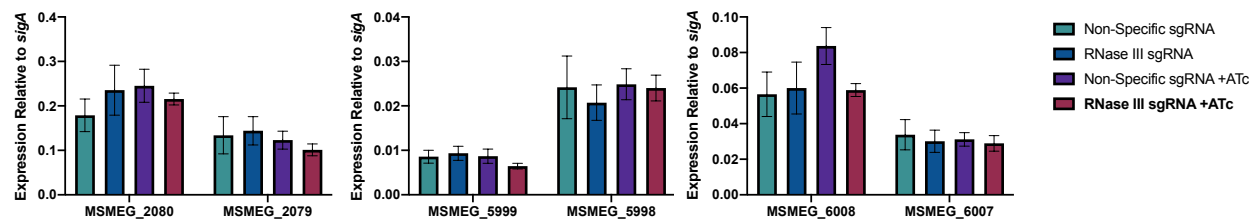


Figure 4: RNase III Knockdown Does Not Affect Expression of Genes Flanking Putative RNase III Cleavage Sites.

Expression of genes flanking potential RNase III cleavage sites was measured by qPCR. Triplicate cultures from the four indicated conditions were harvested 12 hours after addition of ATc or the vehicle. Bars indicate mean and error bars denote standard deviation.

RNase III Affects rRNA Maturation:

RNase III was previously suggested to play a role in rRNA maturation (Taverniti, 2011).

We therefore decided to test the impact of the RNase III knockdown on rRNA processing.

Figure 5 shows one of the two rRNA transcripts in *M. smegmatis* and the potential RNase III cleavage sites as described by Taverniti *et al.*, 2011. The two rRNA operons are identical except for a region of 138 nt at the 5' end of the leader region. RNase III was predicted to cleave these sites because they occur in regions predicted to be double-stranded and because they were not affected by knockdown or deletion of other RNases (Taverniti, 2011).



Figure 5: Overview of the rRNA Operon in *Mycobacterium smegmatis*

This graphic shows the primary rRNA transcript before processing. It contains the 23S, 16S, and 5S subunits (teal arrows) along with spacer regions between them (black lines). The scissors represent the locations of likely RNase III cleavage sites (CS₁, CS₂, CS₃, CS₄) and an RNase E cleavage site predicted by Taverniti *et al.*, 2011. The schematic is not drawn to scale, and the sizes of each part of the transcript are shown below the segment.

We ran total RNA from cultures 18 hours after ATc was added on TBE-agarose gels (Figure 6). The RNA profiles for the control cultures samples appear equivalent and they all have the mature 23S rRNA, a faint band that appears to be a 16S rRNA precursor, and the

mature 16S rRNA. The 5S rRNA was not visualized on this gel. However, for the RNase III sgRNA ATc samples, there was a faint band at the top of the gel above the 23S rRNA at ~5000 bp and the 16S rRNA precursor was not present. Previous testing showed that the top band at ~5000 bp was barely visible in RNA samples 14 hours after ATc was added, but it was much brighter in the 18 hour samples; this suggests that this rRNA precursor accumulates over time as *rnc* expression level decreases.

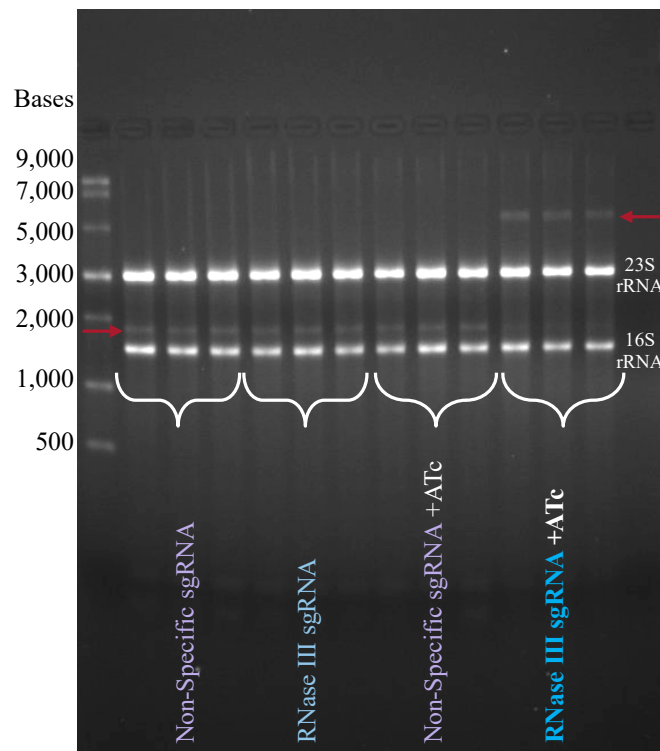


Figure 6: RNA Gel Shows Differences Between Control Samples and RNase III Knockdown.

RNA samples extracted from triplicate cultures 18 hours after ATc was added were run on a TBE-agarose gel. The brightest bands represent the 23S and 16S rRNAs, which are labeled. The red arrows highlight the differences between the controls and the RNase III knockdown mutant. The bases on the left correspond to the RNA ladder run in the first lane.

5' RACE Confirmed the Locations of CS₁ and CS₂:

In order to better understand the role of RNase III in rRNA maturation, we examined the cleavage sites that were previously reported and suggested to be cut by RNase III (Taverniti, 2011). The first step in this process was confirming that there were indeed cleavage sites at the

reported positions. 5' RACE and 3' RACE experiments were used to map the 5' or the 3' ends produced by cleavage at CS₁, CS₂, and CS₃. Figure 8 shows the results of 5' RACE for mapping CS₁, which was expected to produce DNA fragments of 152 bp. As shown in the gel on the left, there was genomic DNA contamination, which resulted in a ~150 nt amplification product from all samples including those that did not have the reverse transcriptase added. The bands in Figure 8A (shown at the size indicated by the red arrow) were excised from the gel and PCR was re-run with nested primers for CS₁. The gel in Figure 8B shows the presence of bands at approximately 112 bp (the expected size of the DNA fragment mapping site 1 with the nested primers) for the reverse transcriptase samples, running just above the genomic DNA contamination bands. Sequencing of the RT-specific bands showed that cleavage was occurring 1 nt upstream of the position previously reported (Taverniti, 2011). This cleavage site was found to be 151 bp upstream of the 5' end of the mature 16S rRNA (Figure 13). The previous report mapped 5' ends by primer extension, which does not always have single-nucleotide precision. It is therefore not surprising to find that the actual cleavage site is slightly different from what was reported.

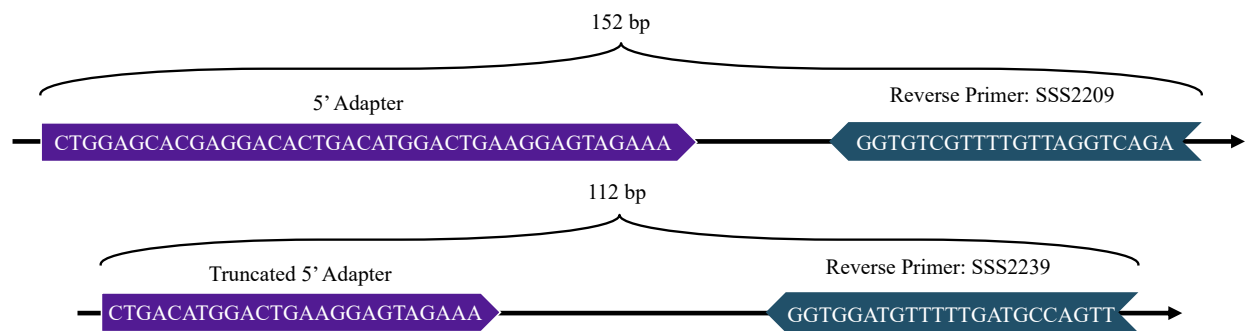


Figure 7: Expected CS₁ Fragment from 5' RACE

The top schematic shows the expected DNA fragment from 5' RACE with the initial primer set. The bottom schematic shows the expected DNA fragment from 5' RACE with the nested primer set.

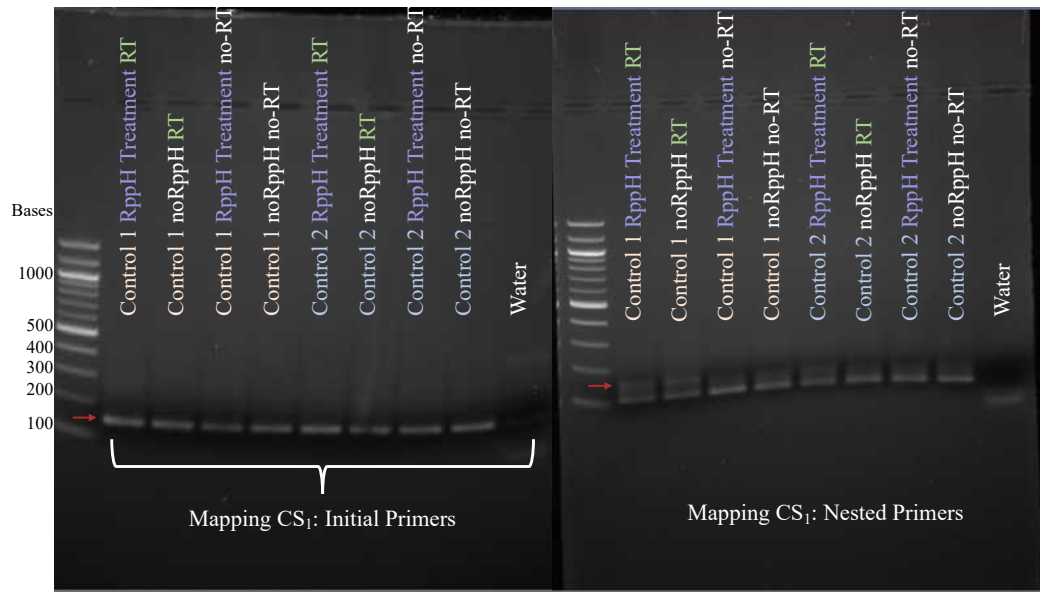


Figure 8: 5' RACE to Map the Location of CS₁

Both images are of 1.5% agarose gels run of the 5' RACE samples run with primers for mapping the expected RNase III CS₁. Control 1 and 2 are replicate cultures of a strain containing a non-targeting sgRNA.

A. The image on the left is the first gel run where genomic DNA contamination was visualized. The red arrow highlights the bands of genomic DNA contamination and misannealing of the primers. **B.** The image on the right is a gel run with nested primers for mapping CS₁ using the DNA extracted from the first gel.

We then used 5' RACE to attempt to map CS₃ (Figures 9 and 10). The faint bands at the bottom of the gel are possibly genomic DNA contamination or primer dimers that formed during the PCR. The bands at ~150 bp seen in the reverse transcriptase samples were excised because they were close to the expected size of 138 bp. The bands at ~250 bp were also excised because we hypothesized they could come from rRNA precursors cleaved at CS₂ (expected size 231 bp). Sequencing revealed that the band predicted to be mapping CS₃ was actually mapping a cleavage site predicted to be made by another enzyme 27 bp upstream of the expected RNase III CS₃ (shown in Figure 9). The Taverniti *et al.*, 2011 paper suggested that this other site was cleaved by RNase E (shown in Figure 5). The DNA fragments for the expected RNase III CS₂ were also sequenced. These fragments showed a cleavage site 212 bp upstream of the 23S rRNA gene (MSMEG_3756), which is consistent with the approximate location of CS₂ as predicted by Taverniti *et al.*, 2011.

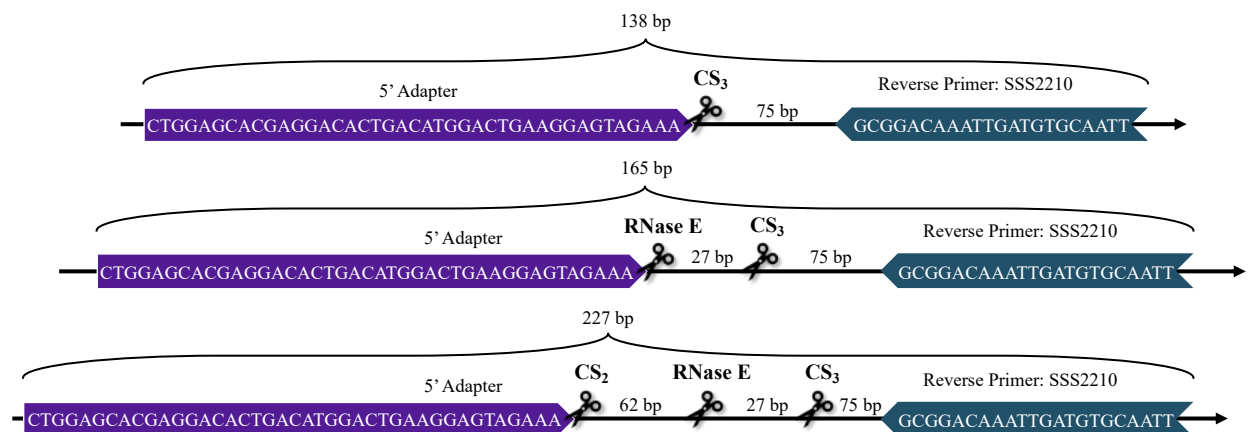


Figure 9: Expected CS₃ Fragment from 5' RACE

The top schematic shows the expected DNA fragment from the 5' RACE if CS₃ is mapped. The bottom two schematics show the DNA fragments that were actually mapped, which correspond to the approximate location of a predicted RNase E cleavage site (middle) and CS₂ (bottom).

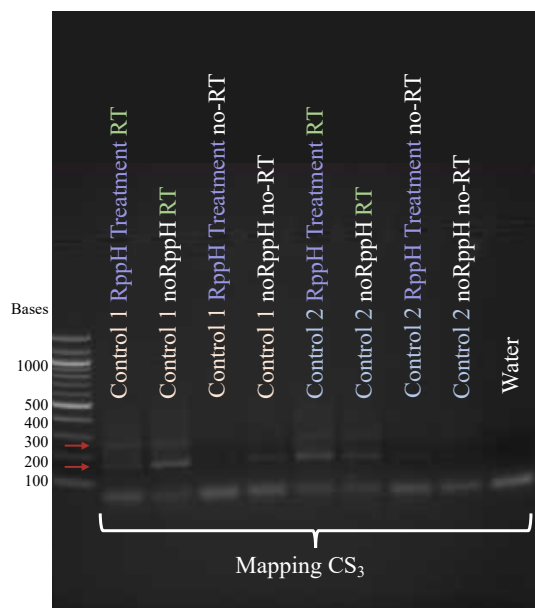


Figure 10: 5' RACE attempting to Map CS₃, and actually mapping a Potential RNase E Cleavage Site and CS₂

This image is of a 1.5% agarose gel of the 5' RACE samples run with primers to map the expected RNase III CS₃. The red arrows mark the bands that were sequenced and shown to be a potential RNase E cleavage site (not the expected CS₃) (the bottom arrow at ~150 bp) and CS₂ (the top arrow at ~250 bp).

3' RACE Further Confirms the Location of CS₂:

3' RACE experiments (Figure 11) were designed in order to study CS₂ because there was predicted to be a longer region of intact RNA upstream of CS₂ than downstream and in Sanger sequencing the first ~100 bp of DNA sequenced are not properly registered. Figure 12 shows the

results of 3' RACE for mapping CS₁ and CS₂. The mapping of CS₁ showed the presence of primer dimers or possible genomic DNA contamination and no bands of the expected size for mapping site 1 (~175 bp). However, the mapping of CS₂ produced bands at ~170 bp only in the samples with reverse transcriptase, suggesting that they represent specific products (Figure 12). The expected size for mapping CS₂ was 176 bp (Figure 11). The DNA from these bands was purified and sequenced. The sequencing results confirmed a cleavage site 212 bp upstream of the 23S rRNA gene (MSMEG_3756) as seen with the 5' RACE sequencing results for this site (Figure 10). Additionally, a sequence for another cleavage site was found mixed with the samples containing the first cleavage site; this cleavage site was 211 bp upstream of the 23S rRNA gene. Since this second cleavage site was seen by 3' RACE but not by 5' RACE, we hypothesize that it may result from exoribonucleolytic processing of the 3' end produced by endonuclease cleavage at position -212 relative to the 5' end of the mature 23S.

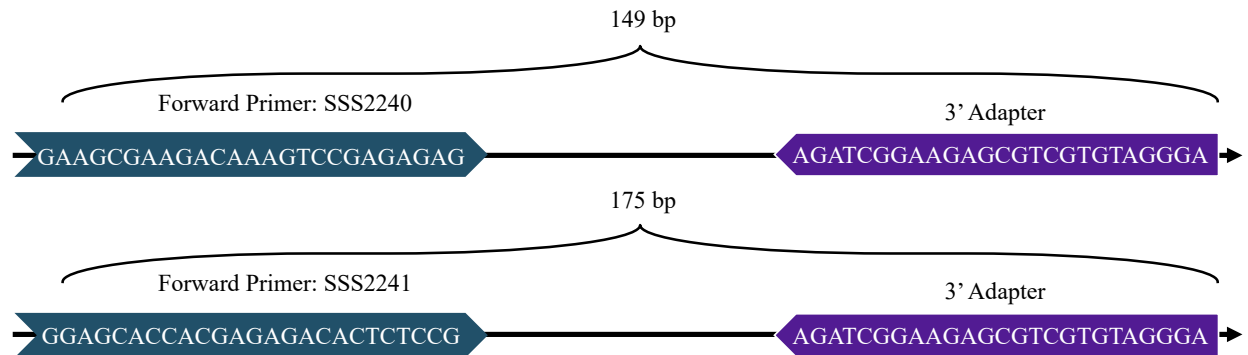


Figure 11: Expected CS₁ and CS₂ Fragments from 3' RACE

The schematic on top shows the expected DNA fragment from the 3' RACE and later PCR for mapping CS₁. The bottom schematic shows the expected DNA fragment from 3' RACE and later PCR for mapping CS₂.

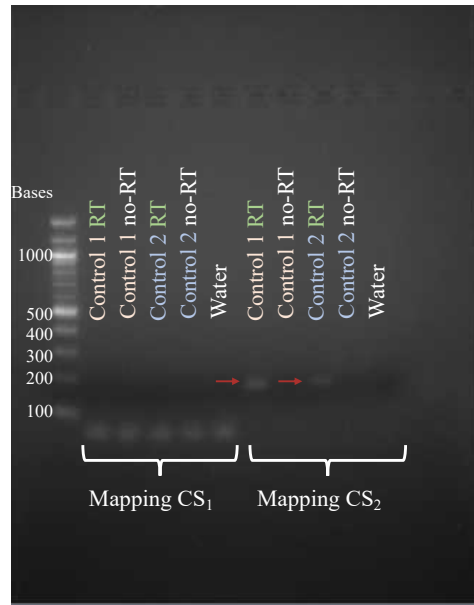


Figure 12: 3' RACE to Map the Location of CS₂

This image is of a 1.5% agarose gel of the 3' RACE samples run with primers to map the expected RNase III CS₁ (on the left) and CS₂ (on the right). The red arrows show the DNA fragments that were extracted, sequenced, and shown to be CS₂.

3' RACE and 5' RACE Reveal the Precise Locations of Possible RNase III Cleavage Sites:

The results of the 3' RACE and 5' RACE experiments were compiled and compared to the predicted cleavage site locations from Taverniti *et al.*, 2011. Figure 13 shows that most of the cleavage sites from Taverniti *et al.*, 2011 are approximately 1-2 nt upstream of the cleavage site locations determined here by Sanger sequencing. This method is far more precise than primer extension assays, which were used by Taverniti *et al.*, 2011 in order to determine the locations of cleavage sites. Our results therefore likely reflect the true cleavage site positions.

Figure 14 shows an overview of the rRNA operon with the known cleavage sites labeled. This data are a mix of the results collected here and the results from the Taverniti *et al.*, 2011 paper. Based on this information, it appears that RNase III may play a role in separating the different rRNAs, which is consistent with rRNA maturation in other bacteria. The cleavage sites studied here have precise data about their locations, but the other cleavage sites from Taverniti *et al.*, 2011 are approximate locations based on primer extension assays.

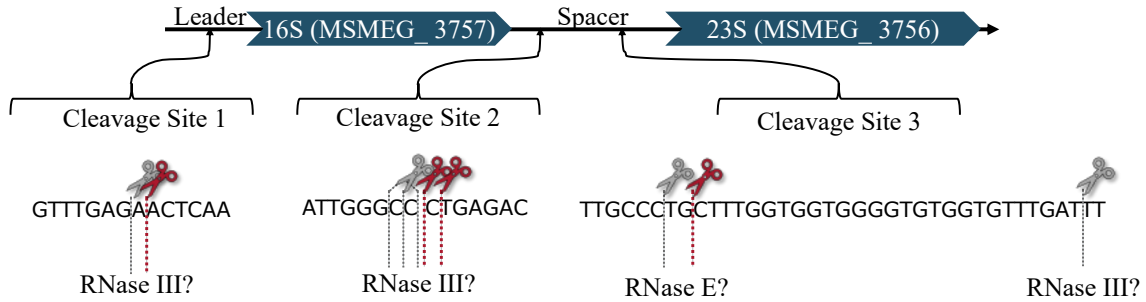


Figure 13: Cleavage Sites Mapped with 3' RACE and 5' RACE Compared to Predicted Cleavage Sites
 The grey scissors represent the cleavage site locations predicted by Taverniti *et al.*, 2011. The red scissors represent the cleavage site locations determined in our study by 3' RACE and 5' RACE and Sanger sequencing. Below each cleavage site is the likely enzyme responsible for the cleavage based on data from Taverniti *et al.*, 2011.

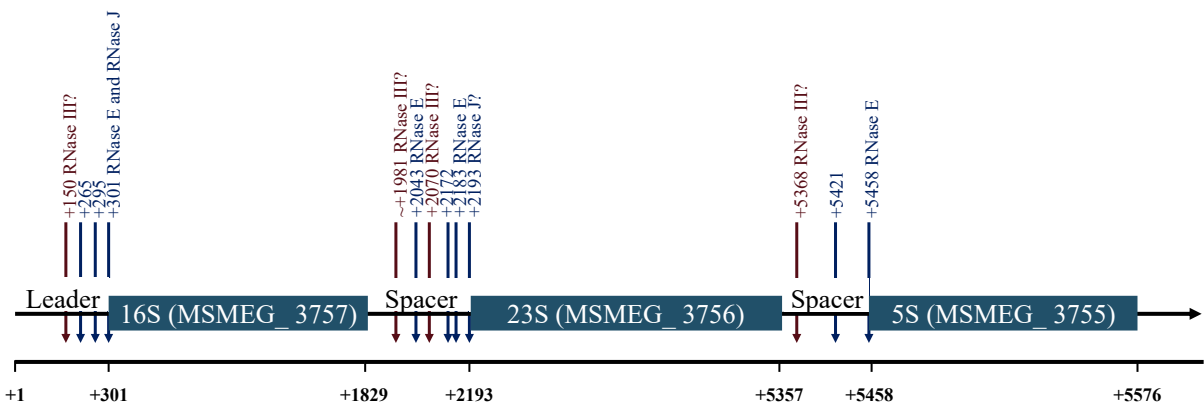


Figure 14: Comprehensive summary of all rRNA Operon Cleavage Sites Mapped here and elsewhere
 This figure represents all the known or predicted cleavage sites in the rRNA operon in *Mycobacterium smegmatis*. The enzymes or likely enzymes (likely enzymes have question marks after their names) that are responsible for each cleavage site are listed above the site (cleavage sites without an enzyme listed above represent sites where the enzyme cleaving the rRNA is unknown). These sites are from the results/data presented here and the results from the Taverniti *et al.*, 2011 paper.

DISCUSSION:

Based on the data collected it is not possible to determine the role of RNase III in mRNA degradation. The expression levels of MSMEG_2080 and MSMEG_2079, MSMEG_5999 and MSMEG_5998, and MSMEG_6008 and MSMEG_6007 did not change when RNase III was knocked down. This suggests that if RNase III is cleaving the regions between these genes, the cleavage does not result in changes to transcript levels. This is consistent with the function of TRIT sequences. TRIT sequences mark the termination of transcription, which suggests that the genes flanking these regions are transcribed separately. Therefore, even if RNase III is involved in cleaving those sites, it is understandable that this would not change the gene expression levels of genes downstream of the TRIT sequence. Further studies of these genes and the expression levels of the entire mRNA pool present in *Mycobacterium smegmatis* will need to be completed in order to understand the direct and indirect effect of RNase III during mRNA degradation.

The RNA agarose gel suggests that when RNase III levels are decreased as a result of the gene being silenced, there is a change in the processing of rRNA. The faint bands at the top of the gel suggest that as RNase III is silenced and RNase III levels start to decrease, there is a buildup of the unprocessed or mostly unprocessed rRNA transcript. This could be due to other enzymes, such as RNase E and RNase J, that are known to process the 23S, 16S, and 5S transcripts into their mature forms, being dependent on the initial RNase III cleavage of the transcript. The Taverniti *et al.*, 2011 paper suggested that RNase III was one of the first enzymes to begin processing the rRNA transcript; in most eubacteria, RNase III or other RNases that cleave double stranded RNA separate the different rRNA precursors before the other RNases process the rRNAs into their mature forms (Taverniti, 2011). The results of the RNA gel appear

to support this order of rRNA processing and suggest that it is the same in *M. smegmatis* as in other eubacteria.

Additionally, the lack of the 16S rRNA precursor in the RNase III KD ATc samples compared to the controls suggests that RNase III is essential for the production of that precursor. Given that this precursor is absent in samples where the long precursor above the 23S (at ~5000 bp) accumulates, it is tempting to speculate that the long precursor is cleaved by RNase III to produce the 16S precursor. It is unclear what this 16S rRNA precursor may include in addition to the 16S rRNA. There are suspected RNase III cleavage sites 151 bases upstream, 152 bases downstream, and ~240 bases downstream of the 16S rRNA; all of these cleavage sites could result in similar precursor 16S rRNA bands so it is unclear exactly which one or ones may be responsible for the precursor. In order to better understand the specific roles of RNase III in the production of these different RNA agarose gel profiles, the bands of interest will need to be excised and their 5' and 3' ends mapped by RACE to determine their identities and determine where RNase III is cleaving the transcripts.

The 5' RACE and 3' RACE experiments suggest that site 1 and 3 are cleavage sites in the rRNA transcript. These cleavage sites were approximately mapped in the Taverniti *et al.*, 2011 paper, but the results of 3' RACE and 5' RACE provide more precise data about the locations of these cleavage sites. Additionally, these experiments suggest that 27 bp upstream of site 3 there is another cleavage site likely cut by RNase E. The Taverniti *et al.*, 2011 paper mapped a cleavage site near this location, which was the result of RNase E; however, the data presented here provides a more precise location of this cleavage site. The sequence motif of the cleavage site matches the RNase E sequence motif that other members of Shell lab have been studying.

Further testing will need to be done in order to confirm whether RNase III is responsible for these cleavage sites (1 and 3) as hypothesized by Taverniti *et al.*, 2011.

The data collected suggest that RNase III plays an important role in rRNA maturation in *Mycobacterium smegmatis*. The specific nature of its role is still being investigated, but it seems probable that RNase III is responsible for the cleavage of site 1 and 2 of the rRNA transcript.

REFERENCES:

- Altuvia, Y., Bar, A., Reiss, N., Karavani, E., Argaman, L., & Margalit, H. (2018). In vivo cleavage rules and target repertoire of RNase III in Escherichia coli. *Nucleic acids research*, *46*(19), 10380-10394.
- Altuvia, S., Locker-Giladi, H., Koby, S., Ben-Nun, O., & Oppenheim, A. B. (1987). RNase III stimulates the translation of the cIII gene of bacteriophage lambda. *Proceedings of the National Academy of Sciences*, *84*(18), 6511-6515.
- Arraiano, C. M., Andrade, J. M., Domingues, S., Guinote, I. B., Malecki, M., Matos, R. G., et al. (2010). The critical role of RNA processing and degradation in the control of gene expression. *FEMS Microbiol. Rev.* *34*, 883–923. doi: 10.1111/j.1574-6976.2010.00242.x
- Bardwell, J. C. A., Regnier, P., Chen, S. M., Nakamura, Y., Grunberg-Manago, M., & Court, D. L. (1989). Autoregulation of RNase III operon by mRNA processing. *The EMBO journal*, *8*(11), 3401-3407.
- Calin-Jageman, I., & Nicholson, A. W. (2003). RNA structure-dependent uncoupling of substrate recognition and cleavage by Escherichia coli ribonuclease III. *Nucleic acids research*, *31*(9), 2381-2392.
- Conrad, C., Rauhut, R., & Klug, G. (1998). Different cleavage specificities of RNases III from Rhodobacter capsulatus and Escherichia coli. *Nucleic acids research*, *26*(19), 4446-4453.
- DeJesus, M. A., Gerrick, E. R., Xu, W., Park, S. W., Long, J. E., Boutte, C. C., Rubin, E. J., Schnappinger, D., Ehrt, S., Fortune, S. M., Sasseti, C. M., & Ioerger, T. R. (2017). Comprehensive essentiality analysis of the Mycobacterium tuberculosis genome via saturating transposon mutagenesis. *MBio*, *8*(1).

- De La Sierra-Gallay, I. L., Zig, L., Jamalli, A., & Putzer, H. (2008). Structural insights into the dual activity of RNase J. *Nature structural & molecular biology*, 15(2), 206.
- Durand, S., Gilet, L., & Condon, C. (2012). The essential function of *B. subtilis* RNase III is to silence foreign toxin genes. *PLoS Genet*, 8(12), e1003181.
- Gardner, P. P., Barquist, L., Bateman, A., Nawrocki, E. P., & Weinberg, Z. (2011). RNIE: genome-wide prediction of bacterial intrinsic terminators. *Nucleic acids research*, 39(14), 5845-5852.
- Gordon, G. C., Cameron, J. C., & Pflieger, B. F. (2017). RNA sequencing identifies new RNase III cleavage sites in *Escherichia coli* and reveals increased regulation of mRNA. *MBio*, 8(2).
- Ji, X. (2008). The mechanism of RNase III action: how dicer dices. In *RNA interference* (pp. 99-116). Springer, Berlin, Heidelberg.
- Kharrat, A. B. E. L. H. A. K. I. M., Macias, M. J., Gibson, T. J., Nilges, M., & Pastore, A. (1995). Structure of the dsRNA binding domain of *E. coli* RNase III. *The EMBO journal*, 14(14), 3572-3584.
- Le Rhun, A., Lécrivain, A. L., Reimegård, J., Proux-Wéra, E., Broglia, L., Della Beffa, C., & Charpentier, E. (2017). Identification of endoribonuclease specific cleavage positions reveals novel targets of RNase III in *Streptococcus pyogenes*. *Nucleic acids research*, 45(5), 2329-2340.
- Lee, Y., Ahn, C., Han, J., Choi, H., Kim, J., Yim, J., ... & Kim, V. N. (2003). The nuclear RNase III Drosha initiates microRNA processing. *Nature*, 425(6956), 415-419.

- Lim, B., Sim, S. H., Sim, M., Kim, K., Jeon, C. O., Lee, Y., ... & Lee, K. (2012). RNase III controls the degradation of corA mRNA in Escherichia coli. *Journal of bacteriology*, *194*(9), 2214-2220.
- Lioliou, E., Sharma, C. M., Caldelari, I., Helfer, A. C., Fechter, P., Vandenesch, F., ... & Romby, P. (2012). Global regulatory functions of the Staphylococcus aureus endoribonuclease III in gene expression. *PLoS Genet*, *8*(6), e1002782.
- Mackie, G. A. (1998). Ribonuclease E is a 5'-end-dependent endonuclease. *Nature*, *395*(6703), 720-724.
- Martini, M. C., Zhou, Y., Sun, H., & Shell, S. S. (2019). Defining the transcriptional and post-transcriptional landscapes of *Mycobacterium smegmatis* in aerobic growth and hypoxia. *Frontiers in microbiology*, *10*, 591.
- Nicholson, A. W. (1999). Function, mechanism and regulation of bacterial ribonucleases. *FEMS microbiology reviews*, *23*(3), 371-390.
- Rock, J. M., Hopkins, F. F., Chavez, A., Diallo, M., Chase, M. R., Gerrick, E. R., Pritchard, J. R., Church, G. M., Rubin, E. J., Sasseti, C. M., Schnappinger, D., & Fortune, S. M. (2017). Programmable transcriptional repression in mycobacteria using an orthogonal CRISPR interference platform. *Nature microbiology*, *2*(4), 1-9.
- Saramago, M., Robledo, M., Matos, R. G., Jiménez-Zurdo, J. I., & Arraiano, C. M. (2018). Sinorhizobium meliloti RNase III: Catalytic Features and Impact on Symbiosis. *Frontiers in genetics*, *9*, 350.
- Smith, I. (2003). *Mycobacterium tuberculosis* pathogenesis and molecular determinants of virulence. *Clinical microbiology reviews*, *16*(3), 463-496.

- Talkad, V., Achord, D., & Kennell, D. (1978). Altered mRNA metabolism in ribonuclease III-deficient strains of *Escherichia coli*. *Journal of Bacteriology*, *135*(2), 528-541.
- Taverniti, V., Forti, F., Ghisotti, D., & Putzer, H. (2011). *Mycobacterium smegmatis* RNase J is a 5'-3' exo-/endoribonuclease and both RNase J and RNase E are involved in ribosomal RNA maturation. *Molecular microbiology*, *82*(5), 1260-1276.
- Verma, A., King, A. K., & Tyagi, J. S. (1994). Functional analysis of transcription of the *Mycobacterium tuberculosis* 16S rDNA-encoding gene. *Gene*, *148*(1), 113-118.
- World Health Organization. (2020) Tuberculosis. Retrieved from: <https://www.who.int/news-room/fact-sheets/detail/tuberculosis>
- Zhang, K., & Nicholson, A. W. (1997). Regulation of ribonuclease III processing by double-helical sequence antideterminants. *Proceedings of the National Academy of Sciences*, *94*(25), 13437-13441.